CHROM. 10,757

A MATHEMATICAL MODEL OF FREE-FLOW ELECTROPHORESIS

JOSEPH A. GIANNOVARIO*, RICHARD N. GRIFFIN and EDWIN L. GRAY

General Electric Co., Space Division, Space Sciences Laboratory, Philadelphia, Pa. 19101 (U.S.A.)

(First received August 17th, 1976; revised manuscript received October 27th, 1977)

SUMMARY

A computerized mathematical model has been developed of a free-flow electrophoresis cell operating under conditions of no convection and no sedimentation of sample. The complex interactions of the various system parameters have been identified and included in this model. Data inputs representing existing equipment have been processed with the theoretical results comparing well with experimental results. Data were also processed for an experimental electrophoresis cell designed to allow optimum resolution and/or sample throughput while operating in a zero *g* environment. Theoretical results are presented along with some experimental ground-based data.

INTRODUCTION

The fact that particles dispersed in a solution could be influenced by an electric field was first described by Lodge[1] in 1886. Six years later, Picton and Linder[2] related their systematic studies of the phenomenon. However, as with most new techniques, there was a dormant period, and it was not until the work of Tiselius[3] in 1937 that electrophoresis began to receive increased attention. The Tiselius method was originally of interest only to biochemists and medical researchers. However, with the introduction of lower cost equipment and advances such as supporting media, biologists, chemists and engineers use the technique for analysis, separation, identification and purification.

During the nineteen fifties and sixties, men such as Barrollier *et al.*[4] and Hannig[5] proposed preparative electrophoretic techniques based on a flowing system in which both the buffer and the sample were continuously admitted to the electrophoresis chamber, with the separated fractions being collected in individual containers. Such electrophoresis systems are now categorized as "free-flow". Because these systems are made thin to minimize convection problems and to maintain stable temperature gradients, the sample fractions are generally distorted due to both hydro-

---

* To whom inquiries or reprint requests should be addressed.

dynamic and electro-osmotic flow profiles. These types of distortion were recognized by Kolin[6] in his magnetically driven electrophoretic separator, and by Strickler and Sacks[7] and Hannig et al.[8] in the usual free-flow electrophoresis systems.

Distortion of the sample bands can be decreased by decreasing the thickness of the sample stream or by increasing the thickness of the electrophoresis cell. In principle the sample stream thickness could approach zero; in practice the thickness is a significant fraction of the cell thickness. An alternative method of obtaining less distorted sample bands is to increase the electrophoresis cell thickness. This would result in "flatter" profiles for both buffer curtain flow and electro-osmotic flow, but would aggravate the problem of convection since the temperature difference would be greater in a thicker cell. A thin cell can be expected to have severe distortion of the sample due to steep flow profiles, while a thick cell will suffer from convection problems.

A solution is possible. Since convection and sedimentation are attributable to a gravity field, these problems may be alleviated, at least theoretically, if the cell system were to be operated in a zero g environment. The advantages would be: a thicker cell to flatten the flow profiles and the absence of convective mixing and sedimentation of samples at high concentration.

This work describes a mathematical model of an electrophoresis cell which operates under the conditions of no convection and no sedimentation (absence of gravitational effects).

THEORETICAL FOUNDATION

General

In electrophoresis the item of interest is the rate of migration. Provided the migration path is of sufficient length a mixture of components may be separated. The rate of migration (electrophoresis) is a function of net charge, size and shape of the particles, and retarding factors such as viscosity. A particle which has no net charge or is uncharged should not migrate. However, a liquid flow occurs, induced by the applied field, which causes all species present to migrate. This is known as electroosmosis.

The following sections will discuss the ζ-potential, electrophoretic velocity and mobility, and electro-osmosis.

ζ-Potential

The charge and potential near a phase boundary have been considered in detail by Debye and Hückel[9], Audubert[10], Gouy[11], Chapman[12], Stern[13] and others. The application of these equilibrium properties to electrokinetics has led to the concept of a "slipping plane" displaced somewhat from the actual phase boundary. Electrokinetic phenomena are controlled by the potential at this slipping plane called the ζ-potential as indicated in Fig. 1. The concept of the slipping plane and its attendant potential is useful in measurements and calculations relating to electrophoresis, but the relationship to more fundamental properties of the phase boundary is somewhat tenuous. More detailed descriptions of ζ-potentials and their application in electrophoresis can be found in refs. 14–17, and in the many references cited therein.
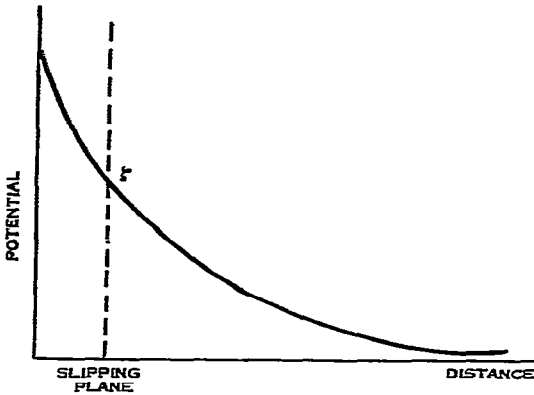
Fig. 1. Variation of potential with distance from a charged surface.

Electrophoresis and mobility

Elementary analysis indicates that if an electric field, $\bar{E}$, is applied to a particle of net charge C, the force producing electrophoretic migration is $\bar{E}C$. The resisting force is given by Stokes' law, i.e., $F = 4\pi a \eta V$ for a spherical particle where a is the particle radius, η is the bulk viscosity of the medium and V is the particle velocity. If the particle has mass m, and neglecting electrostatic interactions, the motion is described by

$$\bar{E}C = \frac{m\mathrm{d}^2 x}{\mathrm{d}t^2} + 4\pi\eta a \frac{\mathrm{d}x}{\mathrm{d}t} \tag{1}$$

The transient response is rather small (10^{-14} sec) and the particle accelerates to its limiting velocity almost instantly. The limiting velocity or the electrophoretic velocity (V_{ep}) is given by:

$$V_{ep} = \frac{\bar{E}C}{4\pi\eta a} \tag{2}$$

The mobility μ (velocity in unit field) is given by:

$$\mu = \frac{V_{ep}}{E} = \frac{C}{4\pi\eta a} \tag{3}$$

and it can be shown that the mobility is related to the ζ-potential in the following manner:

$$\mu = \frac{\zeta D}{4\pi\eta} \tag{4}$$

where D is the dielectric constant of the solution.

It has, of course, been shown that the constant, 4π, in eqns. 1–4 is valid only when the radius of the phase boundary is large compared to the thickness of the

electrical double layer. Under other circumstances the constant can range up to 6π[18,19], depending on particle size and the composition and ionic strength of the surrounding medium. For our present purpose the use of the constant, 4π, will suffice. The extension to other circumstances is obvious.

Electro-osmosis

The phenomenon known as electro-osmosis is due to the potential difference existing between the wall of a chamber and the layer of liquid lying next to it; that is to the double layer at the boundary between solid and liquid. The application of an electric field must cause a displacement of the charged layers, and since the wall cannot move the liquid must, and a flow results. The direction of flow depends on whether the ions in this double layer are positive or negative.

Suppose that the wall of the chamber is negatively charged and the layer of liquid adjacent is positively charged. If a field $\bar{E}$ is applied and the surface density of charge is given by σ the force acting on unit surface is $\bar{E}\sigma$. The viscous forces opposing flow are given by $\eta(V_{eo}/\delta)$ where δ is the double layer thickness and V_{eo} is the electro-osmotic velocity. For a steady flow the two forces must be equal.

$$\bar{E}\sigma = \eta\,\frac{V_{eo}}{\delta} \tag{5}$$

As in electrophoresis, the electro-osmotic velocity at the wall, V_w, can be related to ζ-potential (of the wall) and is given as

$$V_w = \frac{\zeta_w\,D\bar{E}}{4\pi\eta} \tag{6}$$

where D is the dielectric constant of the solution, η is its viscosity and ζ_w is the ζ-potential of the wall surface with respect to the bulk solution. The fundamentals of electro-osmosis in a closed system are well known[19], and while a free-flow electrophoresis system is, by definition, not a closed system it is closed in the direction of electro-osmosis and the recirculation characteristic of a closed system is observed. Nee has recently re-examined in detail the fundamental equations describing electro-osmosis[20].

ASSEMBLY OF THE COMPUTERIZED MODEL

Introduction

A useful electrophoresis system designed to operate in a zero-g environment should be flexible enough to handle some of the very different biological materials which remain unseparated by present terrestrial electrophoretic methods. The resolution necessary to obtain useful material will vary for each species. This implies an electrophoresis unit with considerable operational latitude in sample flow-rate, sample residence time, field potential, wall ζ-potentials and separation resolution.

The entire mathematical model is based on a criterion called the separation resolution and defined as $\Delta\mu$, the minimum difference in sample component mobility which will result in the complete separation of two adjacent sample components by
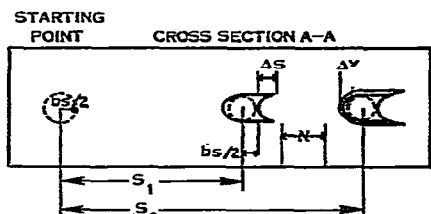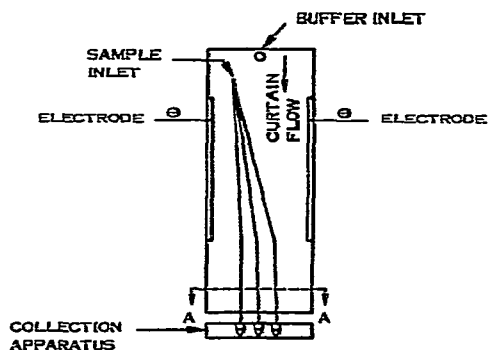
Fig. 2. Schematic, free-flow electrophoresis and definition of separation resolution.

an amount equal to the spacing of the product fraction collection tubes. This is illustrated in Fig. 2.

The term ΔS is the crux of the matter. This term is calculated by taking a sample particle at two locations on the outer edge of the sample stream and calculating net displacements at those points. Fig. 3 illustrates the concept.

The displacement at either point is given by

$$S_x = V_{net(A)} \cdot t_{r(A)} = (V_{ep(A)} + V_{eo(A)}) \cdot t_{r(A)} \qquad (7)$$

$$S_0 = V_{net(B)} \cdot t_{r(B)} = (V_{ep(B)} + V_{eo(B)}) \cdot t_{r(B)} \qquad (8)$$

$$t_r = L/V_b \qquad (9)$$

$$\Delta S = S_x - S_0 = [(V_{ep(A)} + V_{eo(A)}) \, t_{r(A)} - (V_{ep(B)} + V_{eo(B)}) \, t_{r(B)}] \qquad (10)$$
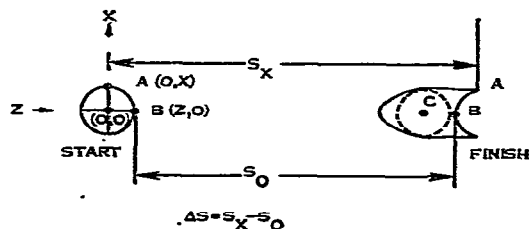

Fig. 3. Definition of sample distortion, ΔS.

where

V_{ep} = electrophoretic velocity,
V_{eo} = electro-osmotic velocity,
V_{net} = algebraic sum of electrophoretic and electro-osmotic velocities,
t_r = residence time in the field,
V_b = the buffer velocity at x and
L = length of the field.

Eqn. 10 is simplified in that it does not take into account diffusion effects. If diffusion were to occur with displacements on the order of the electrophoretic displacements then the A term would be constantly changing during the time particle A is in the field. This effect is built into this model.

In eqn. 10, all of the velocity terms have a dependence upon viscosity, and viscosity is in turn dependent upon temperature. Thus, temperature becomes the most important parameter in the model for separation resolution. Temperature is also important to sensitive (biological) materials, and it is probably necessary to keep the maximum temperature at or below physiological temperature (37°). Therefore, before an attempt can be made to calculate any of the velocities (V_{ep}, V_{eo}, or V_{el}) it is necessary to determine the temperature profile through the cell thickness and the maximum temperature at the cell centerline.

It is now possible to take an overview of the system and identify the interdependence of the cell variables. Fig. 4 shows this interdependence.
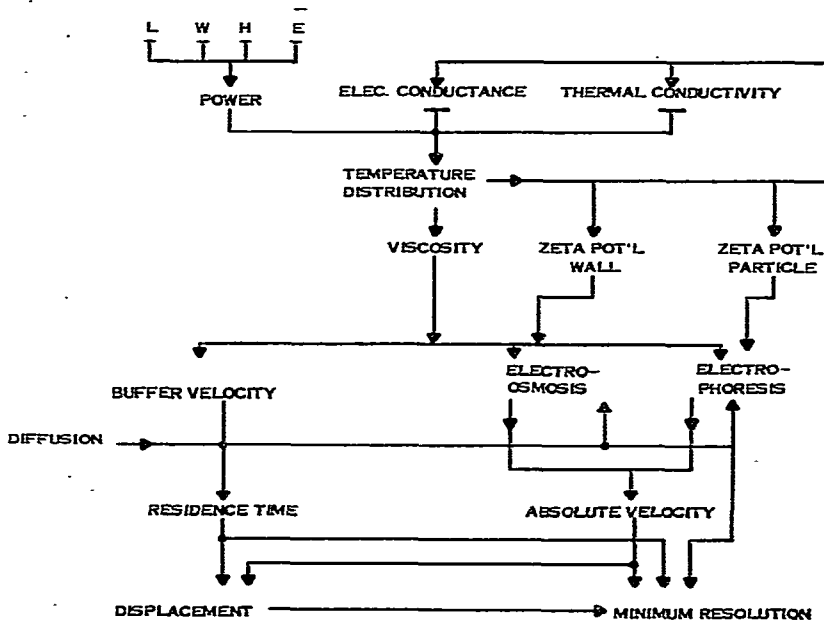

Fig. 4. Interdependence of cell variables.

Temperature distribution and cell thickness: step 1

As mentioned before, it is the cell thickness that is the crucial factor in a successful free-flow system. This is due to several factors: (1) heat transfer occurs through this dimension; (2) the hydrodynamic flow profile is determined by the cell thickness; and (3) the extent of electro-osmotic distortion is determined by the thickness also. The most important parameters here are the temperature distribution and the maximum temperature at the cell centerline. Since these increase rapidly with cell thickness, a trade-off must be made between large temperature gradients and flatter flow profiles.

The first step in the development of the model was to describe accurately the temperature gradient through the cell thickness and from the maximum temperature at centerline to choose an appropriate cell thickness. A similar analysis was performed by Brown and Hinckley[21] subsequent to completion of this work. Their conclusions were generally similar to ours except that we did not consider the wall thickness. In designing equipment we strive for the highest practical thermal conductivity in the walls. Some standard textbook equations were solved first to acquire a "feel" for the solutions (see Figs. 5A, 5B and 6A). Fig. 6B shows the data resulting from the finalized mathematical description of the temperature distribution.
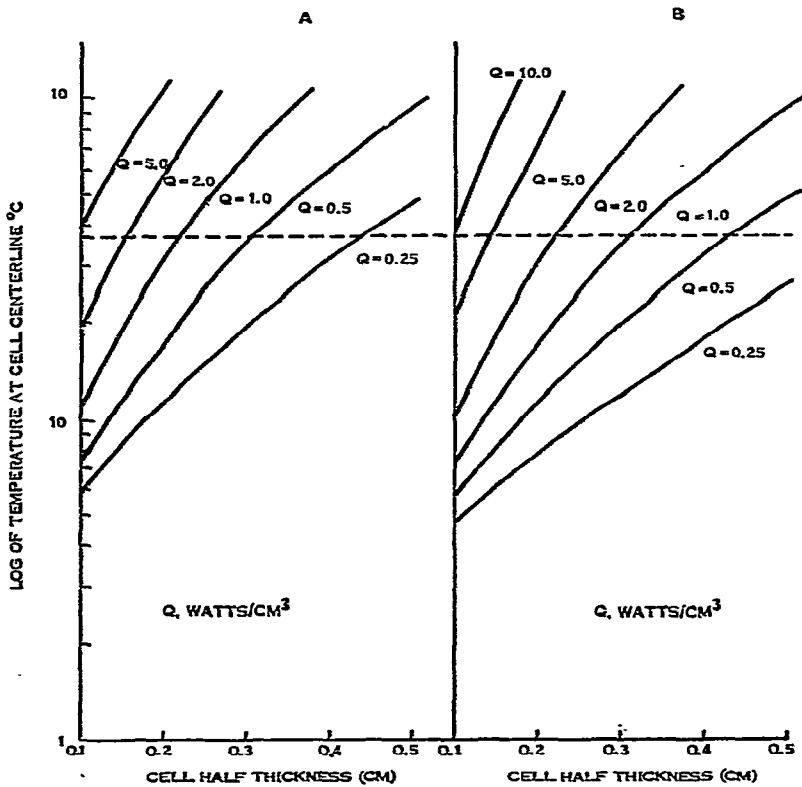

Fig. 5. A, planar heat source; B, distributed heat source, both cases having fixed thermal and electrical conductivities.
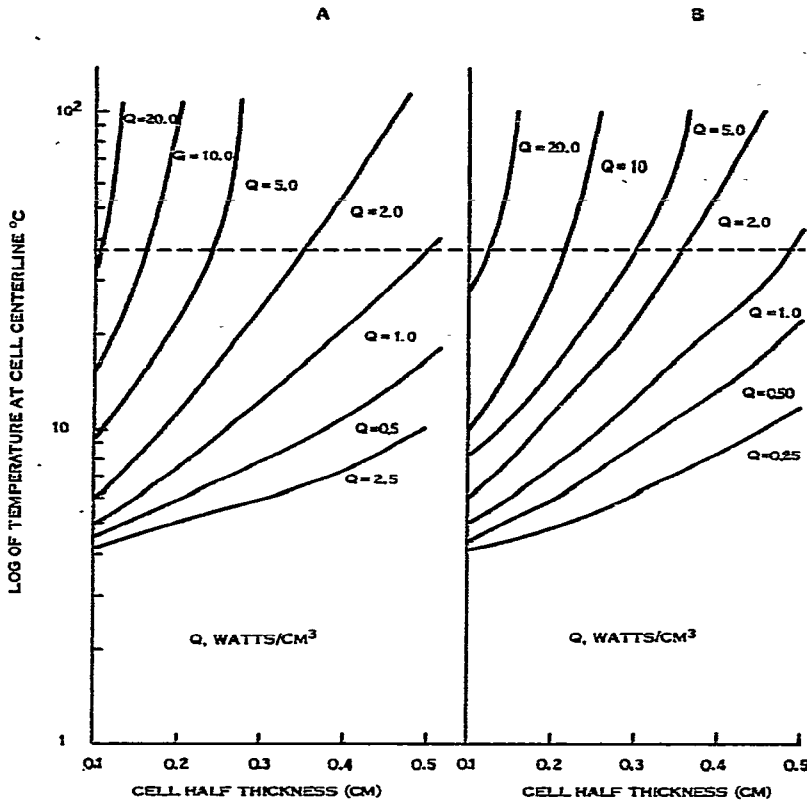
Fig. 6. A, distributed heat source with fixed thermal conductivity and variable electrical conductivity. B, Distributed heat source having variable thermal and electrical conductivity.

The equation governing this distribution may be written as

$$(\alpha + \beta y)\frac{d^2 y}{dx^2} + \beta \left(\frac{dy}{dx}\right)^2 + Q\,(1 + \varepsilon y) = 0 \tag{11}$$

where y = temperature difference from wall at x, x = distance from cell centerline, α = thermal conductivity of buffer at 4°, β = temperature coefficient of the buffer thermal conductivity, ε = temperature coefficient of the buffer electrical conductivity and Q = power density in W/cm³ containing both the field, $\bar{E}$, and the buffer electrical conductivity, ke.

Eqn. 11 is a boundary value problem (of the second kind) rather than an initial value problem. The boundary conditions for eqn. 11 are: the derivative of the temperature at the cell centerline be equal to zero, $y'(0) = 0$ and the temperature difference at the wall (x_f) be equal to zero, $y(x_f) = 0$. The distribution is assumed to be a symmetrical function with respect to the cell centerline. The sought-for value is the temperature at the cell centerline, $y(0)$. Some sort of iterative technique must be used to solve this equation, with the additional condition that the solution converge

reasonably rapidly. The method used here is a variant of the so called "shooting-method", in which a value for $\bar{y}(0)$ is assumed, and with $y'(0) = 0$, the equation is then integrated over $[0,x_f]$, and a $y(x_f)$ is calculated. This result, $y(x_f)$, is compared with the condition $y(x_f) = 0$, and the comparison is used to derive a better estimate of $y(0)$. The process is repeated until successive iterations converge. It is clear that some mechanism must be provided to establish how much $y(0)$ is to be incremented on a given iteration and the Newton-Raphson technique was chosen for this purpose.

Referring to Figs. 5 and 6, note how each refinement of the model has affected the maximum temperatures at the cell centerline. From these data a cell thickness of 0.5 cm (0.25 cm half thickness) was chosen. The horizontal dashed line on each graph represents physiological temperature, 37°. An additional output from this step is the temperature profile through a cell of a given thickness. Figs. 7, 8 and 9 are examples of this output for cells of thickness 0.07 cm, 0.16 cm and 0.5 cm, respectively. These data are read onto a file and used in subsequent calculations.

The data inputs to step one are: buffer conductivity and its temperature coefficient, thermal conductivity and its temperature coefficient, voltage gradient and one-half the cell thickness.
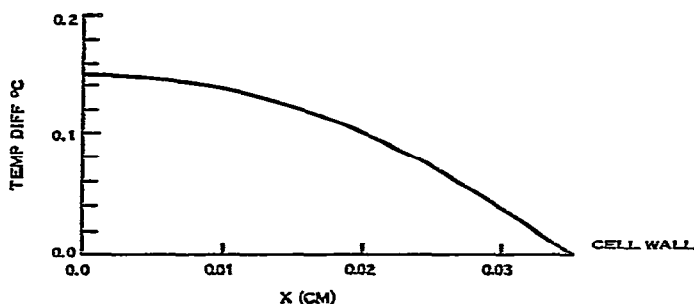

Fig. 7. Temperature gradient vs. distance from cell centerline for a field of 40 V/cm and a conductance of $8.7 \times 10^{-4}\,\Omega^{-1}\,cm^{-1}$. Cell thickness, 0.07 cm.
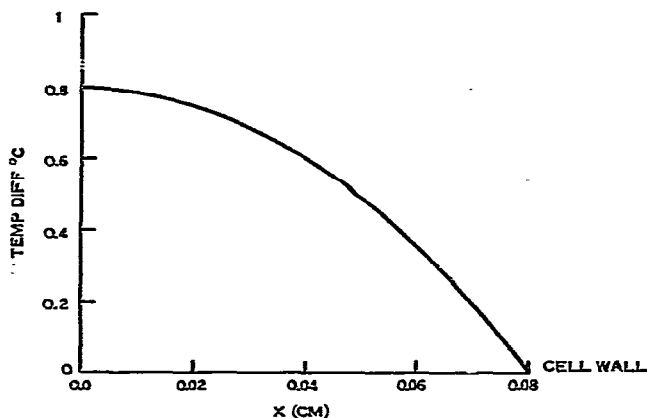

Fig. 8. Temperature gradient vs. distance from cell centerline for a field of 40 V/cm and a conductance of $8.7 \times 10^{-4}\,\Omega^{-1}\,cm^{-1}$. Cell thickness, 0.16 cm.
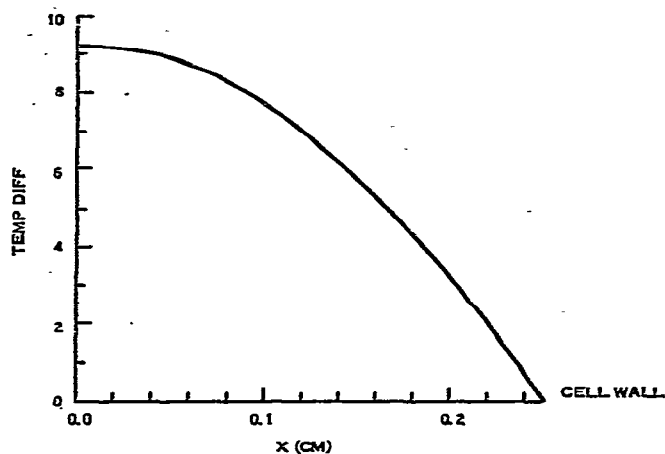
Fig. 9. Temperature gradient *vs.* distance from cell centerline for a field of 40 V/cm and a conductance of $8.7 \times 10^{-4}\,\Omega^{-1}\,cm^{-1}$. Cell thickness, 0.50 cm.

Curtain velocity profile: step 2

The linear velocity of the buffer curtain determines the residence time, t_r, of a particle in the electric field, and therefore determines, in part, the lateral displacement of the particle. In a constant temperature system, the velocity profile would be parabolic due only to viscous friction. However, viscosity decreases with increasing temperature (for a liquid) and since there is a distribution of temperature in the cell, a distortion of the parabolic flow profile results. It is important to know the buffer velocity at all points through the cell thickness, since a sample stream has a finite diameter and therefore particles at the outer edge of the stream move with a lower velocity than particles at the center. The slower parts of the stream have longer residence times and therefore experience different lateral electrophoretic displacements. This ultimately affects resolution.

The equation used to model the flow profile in the cell can be written as:

$$\frac{\partial}{\partial x}\left(\eta \frac{\partial V_b}{\partial x}\right) + \frac{dP}{dz} = 0 \tag{12}$$

where η is the viscosity of the buffer, dP/dz is the pressure gradient causing flow, V_b is the linear buffer velocity at x, a distance from the cell centerline.

Since it is not practical to measure dP/dz in a real system, this quantity must somehow be related to the volumetric flow-rate of the system, a quantity easily measured and controlled. This quantity dP/dz can be written as:

$$-\frac{dP}{dz} = \frac{\bar{\eta}4F}{(4/3)\,ab^3 - (\delta/b)\,\sum_{n=0}^{\infty} N_n^{-5}\tanh N_n a} \tag{13}$$

$$N_n = (2n + 1)\pi/2b \tag{14}$$

where $\bar{\eta}$ is the average viscosity, a and b are one-half of the cell width and thickness, respectively, and F is the volumetric flow-rate[22].

Figs. 10, 11 and 12 show the outputs for cells 0.07, 0.16 and 0.5 cm thick, respectively. The flow-rates in all three cases were adjusted to give comparable residence times in each cell.

The inputs to step 2 are: flow-rate, cell width, cell thickness and temperature points from the data file created in step 1 to calculate variations in viscosity.

Profile of electro-osmotic velocity: step 3

Electro-osmosis occurs normal to the direction of hydrodynamic flow. Since the cell is a closed system in the direction of electro-osmosis, this flow must be recirculating. Depending upon the sign and magnitude of the applied field and the ζ-potential at the wall, this electro-osmotic flow affects the lateral displacement of a particle undergoing electrophoresis. It is necessary to know the profile of this flow, so that a net horizontal displacement can be calculated for particles at various positions in the cell.
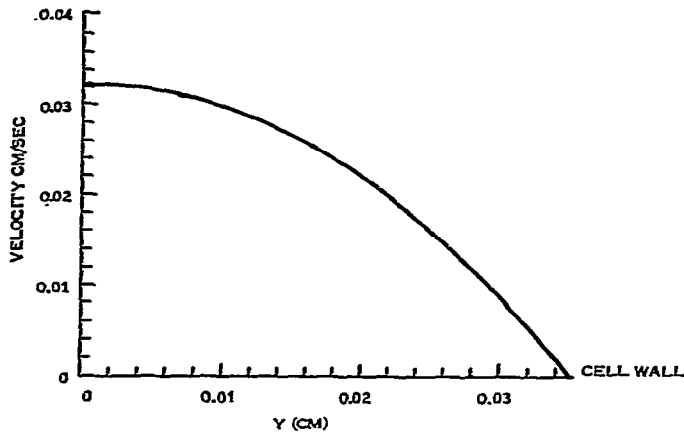

Fig. 10. Buffer curtain velocity *vs.* distance from cell centerline. Cell thickness, 0.07 cm.
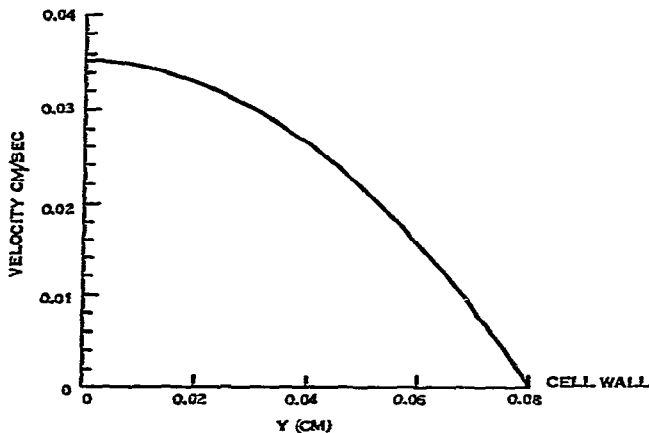

Fig. 11. Buffer curtain velocity *vs.* distance from cell centerline. Cell thickness, 0.16 cm
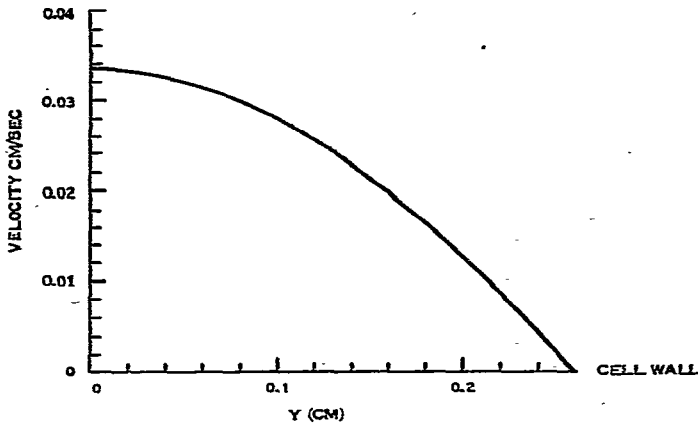
Fig. 12. Buffer curtain velocity *vs.* distance from cell centerline. Cell thickness, 0.50 cm.

The equation used to derive this profile is almost identical to that in step 2 and is written as:

$$\frac{\partial}{\partial x}\left(\eta\,\frac{\partial V_{eo}}{\partial x}\right) + F = 0 \tag{15}$$

where η is the viscosity, V_{eo} is the electro-osmotic velocity at distance x from the cell centerline and F is the driving force for electro-osmotic flow. An expression is needed to relate the ζ-potential of the wall to the force driving the fluid. If an average viscosity is assumed, then eqn. 15 becomes

$$-F = \bar{\eta}\,\frac{d^2\,V_{eo}}{dx'^2} \tag{16}$$

and reduces to

$$V_{eo} = \frac{Fx'^2}{2\bar{\eta}} + C_1\,x' + C_2 \tag{17}$$

If the cell is described through its thickness as shown in Fig. 13, the boundary conditions are at $x' = 0$; $V_{eo} = V_w$. At $x' = s$, $V_{eo} = V_w$, so that eqn. 17 becomes:
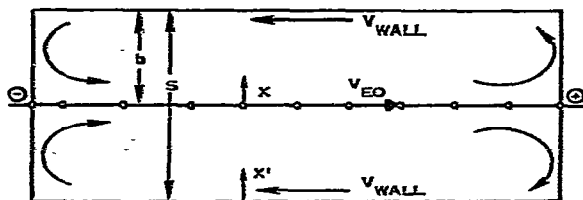
$$V_w = -\frac{F(0)^2}{2\bar{\eta}} + C_1(0) + C_2 \tag{18}$$

so that $C_2 = V_w$ and

$$V_w = -\frac{F(s)^2}{2\bar{\eta}} + C_1(s) + V_w \tag{19}$$

so that

$$C_1(s) - \frac{F(s)^2}{2\bar{\eta}} = 0 \tag{20}$$

b=HALF THICKNESS = 1/2 S
X=O AT CENTERLINE
Y=O AT BOTTOM WALL; Y= S AT TOPWALL

Fig. 13. Closed-flow electro-osmosis.

and

$$C_1 = \frac{Fs}{2\bar{\eta}} \tag{21}$$

It follows that eqn. 15 is now transformed to

$$V_{eo(x')} = -\frac{Fx'^2}{2\bar{\eta}} + \frac{Fsx'}{2\bar{\eta}} + V_w \tag{22}$$

From Smoluchowski's equation for a rectangular cross section cell:

$$V_{eo(x)} = V_w - 6\,V_w\left(\frac{x's - x'^2}{s^2}\right) \tag{23}$$

Setting equations 22 and 23 equal:

$$-6\,V_w\left(\frac{x's - x'^2}{s^2}\right) = \frac{F}{2\bar{\eta}}(x's - x'^2) \tag{24}$$

$$-\frac{6\,V_w}{s^2} = \frac{F}{2\bar{\eta}} \tag{25}$$

$$F = -\frac{12\,V_w\,\bar{\eta}}{s^2} \tag{26}$$

Since $s = 2b$

$$F = -\frac{3\,V_w\,\bar{\eta}}{b^2} \tag{27}$$

From eqn. 6

$$V_w = \frac{\zeta_w\,D\bar{E}}{4\pi\eta} \tag{28}$$

Substituting into eqn. 27, the result is:

$$F = -\frac{3}{4}\frac{\zeta_w\,D\bar{E}}{\pi b^2} \tag{29}$$

where D is dielectric constant, $\bar{E}$ is field, b is 1/2 cell thickness and ζ_w is the ζ-potential. Now eqn. 15 can be written as:

$$\frac{3}{4}\frac{\zeta_w}{\pi b^2} = \frac{\partial}{\partial x}\left(\eta\,\frac{\partial V_{eo}}{\partial x}\right) \tag{30}$$

This last equation is the one used to calculate the final electro-osmotic velocity profile in the cell. Figs. 14, 15 and 16 are the results of these calculations for cells of 0.07, 0.16 and 0.5 cm thickness, respectively. Note that in each case there is a point at which V_{eo} is zero, and beyond that the flow direction reverses. This correlates well with the "real world" situation.
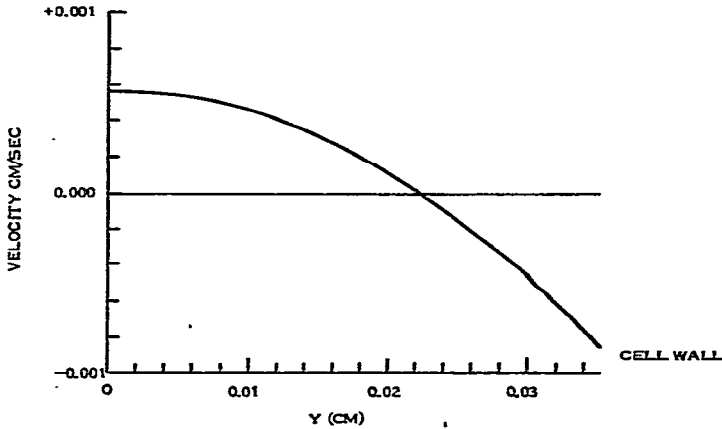

Fig. 14. Electro-osmotic velocity (V_{eo}) vs. distance from cell centerline for a field of 40 V/cm and a wall ζ-potential of 5 mV. Cell thickness, 0.07 cm.

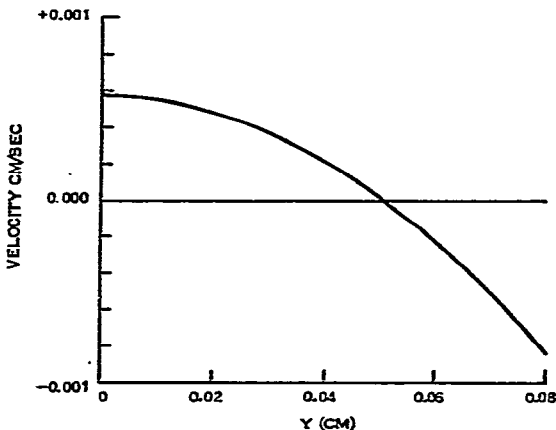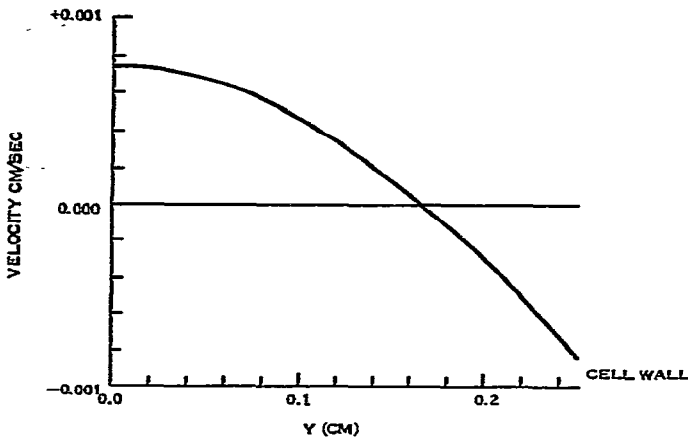Fig. 15. Electro-osmotic velocity (V_{eo}) vs. distance from cell centerline for a field of 40 V/cm and a wall ζ-potential of 5 mV. Cell thickness, 0.16 cm.

Fig. 16. Electro-osmotic velocity (V_{eo}) vs. distance from cell centerline for a field of 40 V/cm and a wall ζ-potential of 5 mV. Cell thickness, 0.50 cm.

Inputs to step 3 are: ζ-potential of the wall surface, dielectric constant of the buffer, the field gradient, 1/2 cell thickness and the temperature from the data file created in step 1 to calculate the variation in viscosity.

Diffusion effects and residence time (t_r): step 4

Depending on the kinds of particles in the sample stream and on the residence time within the field, diffusion effects may play an important role in the separation and resolution achieved. Diffusion will cause the sample stream to increase in diameter as it traverses the length of the cell. If the diffusion time is short compared to the residence time, sample particles will move into slower curtains and the residence times will increase. The effect of diffusing into a slower stream can be compared to a decelerating force and the increase in residence time can be calculated by using the following equation:

$$L = V_0 t_r - 1/2 A t_r^2 \tag{31}$$

where L is the length of the electrophoresis cell, V_0 is the initial velocity of a particle at the outer edge of the sample stream, A is the change in velocity with respect to time (due to diffusion) and t_r is the residence time.

The effect of diffusion can be related to eqn. 31 in the following manner: if the mean increase in sample diameter is expressed as[23]

$$\overline{\Delta r} = (6 D_1 t)^{1/2} \tag{32}$$

where D_1 is the diffusion coefficient and t is time, then the change in ΔV with respect to time is given as

$$\frac{d\Delta r}{dt} = \left(\frac{3}{2} \frac{D_1}{t}\right)^{\frac{1}{2}} \tag{33}$$

Since Δr in this case corresponds to a change in x, the position through the thickness, it is possible to substitute dx/dt for $d\Delta r/dt$. Now, acceleration or deceleration in this case is defined as

$$a = \frac{dV}{dt} \tag{34}$$

However, with a change of variables

$$a = \frac{dV}{dx} \frac{dx}{dt} \tag{35}$$

or

$$\frac{1}{2} a t^2 = \frac{1}{2} \frac{dV}{dx} \left(\frac{3D_1}{2t}\right)^{\frac{1}{2}} t^2 \tag{36}$$

from eqn. 35. Rearrangement brings

$$\frac{1}{2} at^2 = \frac{1}{2} At^{3/2} \tag{37}$$

where

$$A = \frac{dV}{dx} \left(\frac{3D_1}{2}\right)^{1/2} \tag{38}$$

Starting with the initial estimate of $t_r = L/V_0$ a distance is calculated from eqn. 31 and compared to L, the actual length of travel. Using the Newton-Raphson routine an increment, DEL, is generated and added to the old residence time and the cycle begins again until the difference between the calculated distance and the actual distance meets the convergence criterion.

Table I contains the data obtained for three cells of thickness 0.07, 0.16 and 0.5 cm.

TABLE I

RESIDENCE TIME t_r AT EDGE OF SAMPLE STREAM

In all cases $L = 10.16$ cm and $D_1 = 5 \times 10^{-9}$ cm²/sec.

Parameter	Value		
Thickness (cm)	0.07	0.16	0.50
V_0 (cm/sec)	0.008	0.030	0.033
A (cm/sec²)	−1.576	−0.331	−0.033
t_r 1st guess (sec)	1163	335	307
1st iteration	1679	338	308
2nd iteration	1720	converges	converges
3rd iteration	1721	converges	converges
ΔX (cm)	0.007	0.003	0.003

For particle remaining at the cell centerline, the residence time is simply the length, L, divided by the curtain velocity at $x = 0$.

The inputs to step 4 are: active cell length, buffer velocity at the edge of the sample stream ($bs/2$) (from step 2), the deceleration factor, A (from step 2), and the diffusion constants of the particles.

Total lateral displacement due to electrophoresis and electro-osmosis: step 5

The total lateral displacement of a particle in the field is the result of electrophoresis, electro-osmosis and residence time. In step 5, the net lateral velocities for the particles at points A and B in Fig. 3 are calculated. For the particle at point B, the net velocity is simply the sum of the electrophoretic and electro-osmotic velocities at $x = 0$. This sum times the residence time at $x = 0$ will yield S_0, the lateral displacement at $x = 0$. Calculation of the similar term, S_x, for the particle at point A, involves integrating the electrophoretic velocity, V_{ep}, and the electro-osmotic velocity, V_{eo}, over the increase in sample diameter. S_x can be written as

$$S_x = \int_0^{t_r} \left\{ V_{ep}(x_{(t)}) + V_{eo}(x_{(t)}) \right\} dt \tag{39}$$

where $x_{(t)} = bs/2 + (6D_1 t)^{1/2} = bs/2 + \Delta x$ ($bs/2$ is the sample stream radius). The boundary conditions on $x_{(t)}$ are: when $t = 0$, $x_{(t)} = bs/2$ and when $t = t_r$, $x_{(t)} = bs/2 + \Delta x$, and from eqn. 35 $dx/dt = ([3/2] [D_1/t])^{1/2}$. The following substitution can be made:

$$dt = \frac{2 (x - bs/2)}{6D_1} dx \tag{40}$$

From eqn. 39 and with a change in the limits of the integration, S_x can be written as:

$$S_x = \frac{1}{3D_1} \int_{bs/2}^{bs/2 + \Delta x} \left\{ V_{ep(x)} + V_{eo(x)} \right\} \left\{ x - \frac{bs}{2} \right\} dx \tag{41}$$

The inputs to step 5 are the diffusion constant of the particle, the sample radius increase and the residence time. The electro-osmotic velocity is taken as necessary from the data file created in step 3. The electrophoretic velocity is calculated from viscosity variations due to temperature gradient, and particle zeta potential.

Minimum resolution: step 6

Going back to Fig. 2, the separation resolution $\Delta\mu$ can now be calculated from the data available:

$$\Delta\mu = \Delta S + N + \Delta x' + bs/2 \tag{42}$$

where $\Delta\mu$ is the minimum difference in sample mobility which will result in the complete separation of two sample components, N is the collection tube spacing,

$\Delta x'$ is the adjacent sample increase in radius due to diffusion and $bs/2$ is the original sample stream radius. ΔS, which is a measure of the sample distortion, is calculated from step 5 data by taking $\Delta S = S_x - S_0$. The absolute minimum is determined by two factors alone, the initial sample stream radius and the collection tube spacing, since it is conceivable to have a case where ΔS and $\Delta x'$ are both zero.

APPLICATION AND RESULTS

Several realistic, yet hypothetical, cases were examined with the completed model. A sample containing four components was theorized. These components had ζ-potentials of 25, 29, 30 and 34 mV, corresponding to the mobilities measured for the fixed red blood cells of chicken, human A, human B and dog, respectively. In each case, the active cell width and length are 5.08×10.16 cm. The thickness was varied. The flow-rate through each cell was adjusted so that a particle at the centerline would have a residence time comparable to the other cases. The sample stream diameter, 0.06 cm, the wall ζ potential, 5 mV, and the field, 40 V/cm, were the same in all cases.
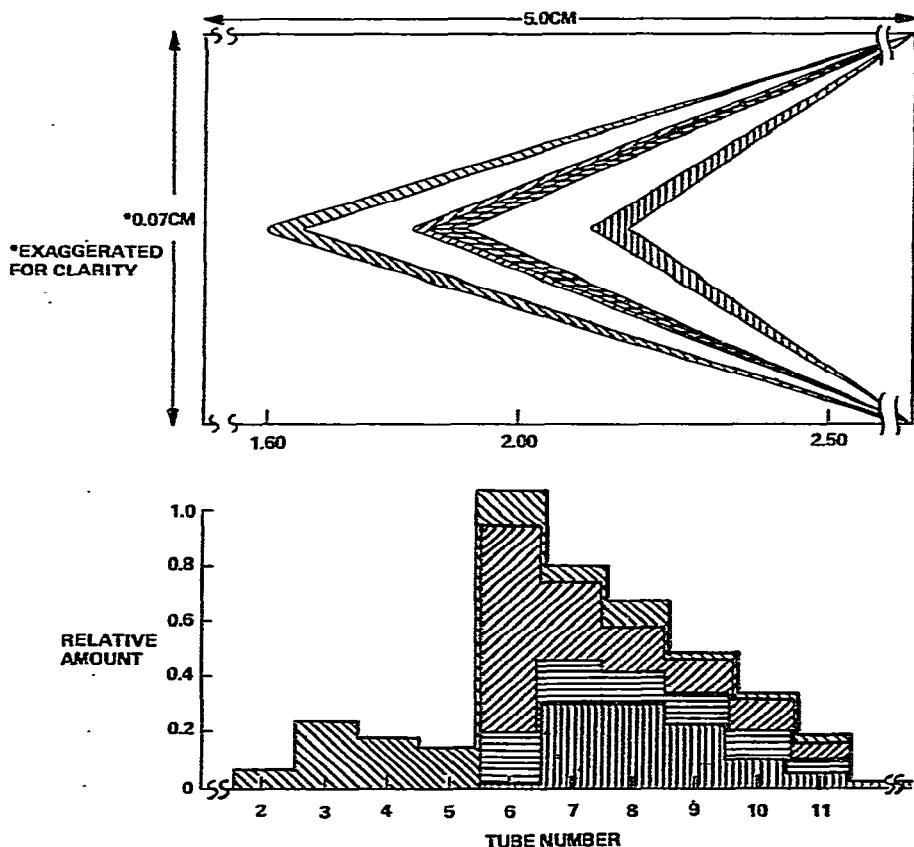

Fig. 17. Graphic illustration of separation and resolution for a 4-component mixture. Cell, 10×5 cm; thickness, 0.07 cm; sample diameter, 0.06 cm; field, 40 V/cm; wall potential, 5 mV; particle potential, 25, 29, 30 and 34 mV; centerline velocity, 0.032 cm/sec.
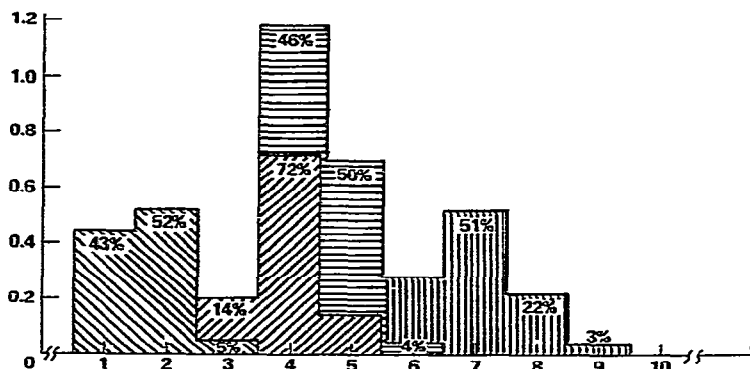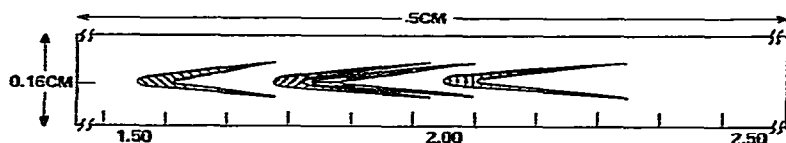
Fig. 18. Graphic illustration of separation and resolution for a 4-component mixture. Cell, 10 × 5 cm; thickness, 0.16 cm; sample diameter, 0.06 cm; field, 40 V/cm; wall potential, 5 mV; particle potential, 25, 29, 30 and 34 mV; centerline velocity, 0.035 cm/sec.

Figs. 17, 18 and 19 are the results of these calculations for cells of 0.07, 0.16 and 0.5 cm thickness, respectively.

The first case, a 0.07-cm thick cell (Fig. 17), is very close to the thickness of the electrophoresis cells described by Barrollier et al.[4] and Hannig[5]. The effects of electro-osmosis and the buffer profile are profound. In addition, referring to Table I, the very long residence time for particles at the outer edge of the sample stream has caused the sample stream to diffuse to the cell walls even though a very small diffusion constant was used, ca. 10^{-9}. The result of moving to the wall is that the particles are now caught in the reverse flow caused by electro-osmosis and further remixing of the sample occurs. As can be seen from the collection graph, no separated material can be collected in any large amount.

The second case, a 0.16-cm cell (Fig. 18), is similar to equipment used in this laboratory. The crescent effect is still quite pronounced and it is still not possible to obtain a complete separation between any of the components.

The last case, 0.5 cm (Fig. 19), is a proposed "thick" zero g experiment cell. A cell of this dimension cannot sustain the resultant temperature gradient in a 1g environment without convection setting in rapidly. Although the crescent effect is still present, it is greatly reduced and it now becomes possible to obtain two components of 100% purity. Of the other two components, 95% of one component can be collected free of other material, while the fourth will contain some 4% (of the total amount) contamination.

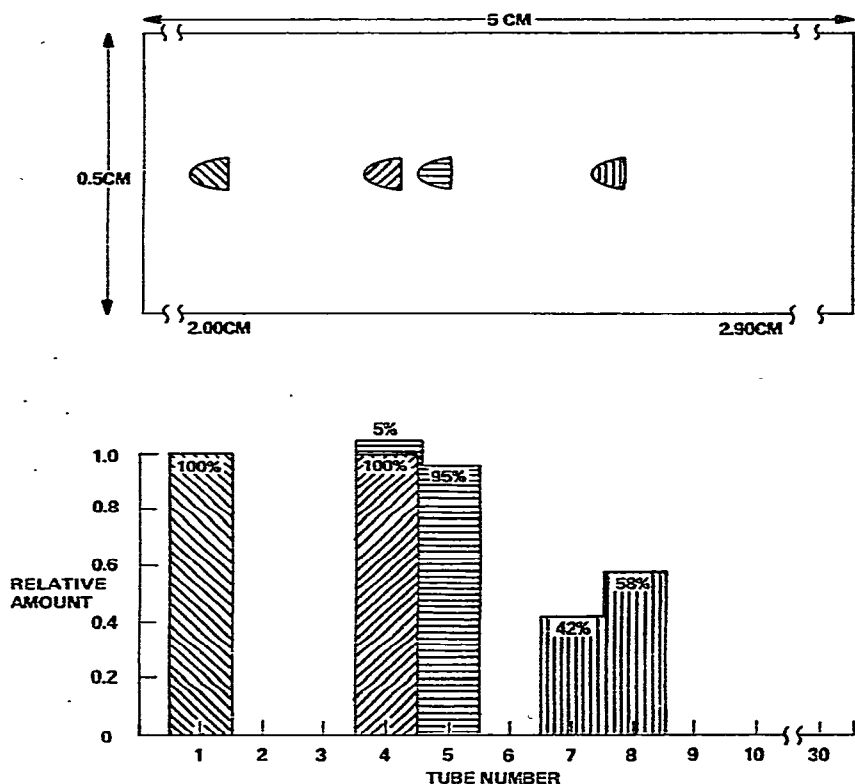In all three cases the ζ-potential of the wall was assumed to be 5 mV. This

Fig. 19. Graphic illustration of separation and resolution for a 4-component mixture. Cell, 10×5 cm; thickness, 0.5 cm; sample diameter, 0.06 cm; field, 40 V/cm; wall potential, 5 mV, particle potential, 25, 29, 30 and 34 mV; centerline velocity, 0.033 cm/sec.

would result in very little electro-osmotic flow and the bulk of the crescent effect is due to the buffer flow profile.

The crescents, in these cases, point from right to left, indicating that particles at the outer edge of the sample stream had more lateral electrophoretic displacement due to longer residence times.

If the wall ζ-potential is changed, for example from 5 to 50 mV, by some treatment of the wall surface, the results would look like Fig. 20. The other parameters are unchanged from case 3. The crescent is now pointing from left to right due to the increased influence of electro-osmosis. Overall, the electro-osmotic velocity at any point is greater than the electrophoretic velocity. As a result, the entire sample band moves farther than previously and particles near the centerline move farther than others in the stream.

Table II lists some data pertaining to these examples. The distortion, ΔS, is given and the separation resolution, $\Delta\mu$, is given in both $\mu m \cdot cm \cdot V^{-1} sec^{-1}$ and in mV.

The first two examples were modeled after existing equipment to check the reliability of the predictions made with the mathematical model. The last two cases are, at present, unable to be verified experimentally, since they require a "zero g" environment. An electrophoresis cell of the dimensions stated for cases 3 and 4 has
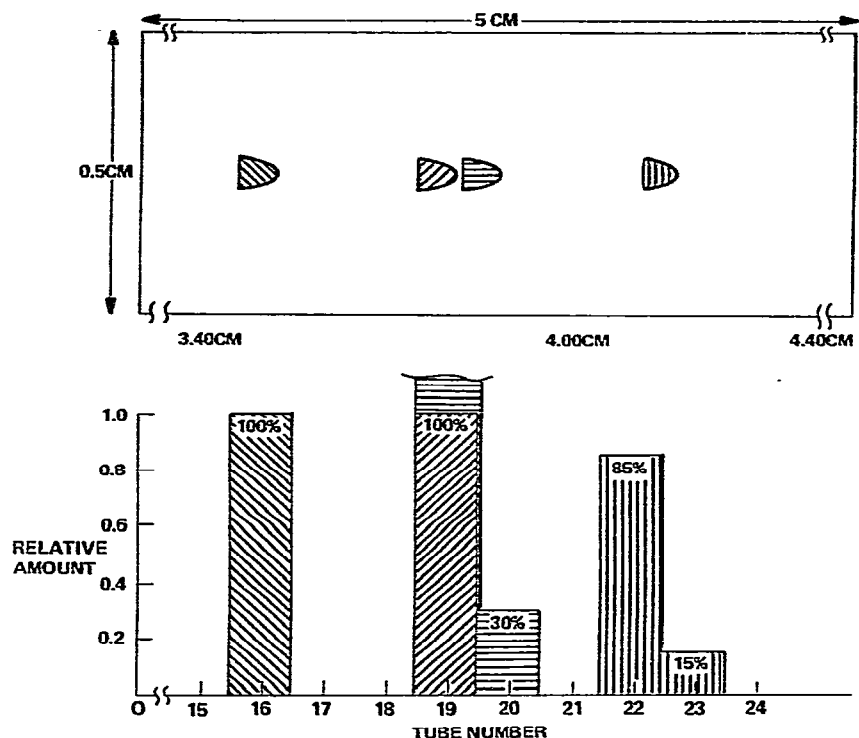
Fig. 20. Effect of a change in the wall ζ-potential. Conditions are the same as in Fig. 19 except the wall ζ-potential has been increased by a factor of 10.

TABLE II

HYPOTHETICAL ELECTROPHORETIC SEPARATIONS

$\Delta S = \text{cm}$

$\Delta \mu = \mu\text{m} \cdot \text{cm} \cdot \text{V}^{-1} \cdot \text{sec}^{-1}$

Separation parameters	ζ-potential				Other parameters
	25 mV	29 mV	30 mV	34 mV	
ΔS	4.96	6.00	6.27	7.31	0.07 cm thick; $\zeta_w = 5$ mV
$\Delta \mu$	4.08	4.89	5.11	5.94	
$\Delta \zeta$ (mV)	78.77	94.42	98.66	114.69	
ΔS	0.19	0.23	0.24	0.27	0.16 cm thick; $\zeta_w = 5$ mV
$\Delta \mu$	0.28	0.31	0.32	0.35	
$\Delta \zeta$ (mV)	5.41	5.98	6.17	6.75	
ΔS	0.024	0.026	0.027	0.032	0.50 cm thick; $\zeta_w = 5$ mV
$\Delta \mu$	0.137	0.137	0.137	0.137	
$\Delta \zeta$ (mV)	2.645	2.645	2.645	2.645	
ΔS	0.034	0.029	0.028	0.024	0.50 cm thick; $\zeta_n = 50$ mV
$\Delta \mu$	0.138	0.137	0.137	0.137	
$\Delta \zeta$ (mV)	2.664	2.645	2.645	2.645	

been constructed and some ground-based data were obtained. These data were then compared to data for thinner cells and then extrapolated to thicker cells. Fig. 21 relates these data, power density, residence time and cell thickness to an arbitrary stability standard. This standard was defined as: an undisturbed flow of neutral density polymer latex for a minimum of 3 min with the field applied. The result is the curved surface shown in Fig. 21. In a 1*g* environment stable operation of the system will occur only for points lying below the surface. Operation at the surface or above it suggests a reduction in the gravity field to decrease convection.
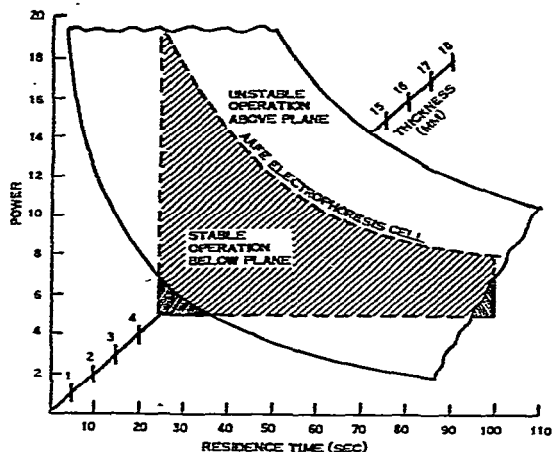

Fig. 21. Experimentally determined regions of stable and unstable operation of an electrophoresis cell as a function of the power (in W) and the residence time for a 0.50-cm thick cell with other conditions as indicated.

Sedimentation of sample at high concentrations is another problem experienced by early researchers. In a preparative system sample throughput would be of prime concern. One solution to the sedimentation problem is to operate the system vertically. However, this orientation tends to maximize convection. Again, a reduced gravity field would serve to overcome these problems. Data were obtained for existing equipment and extrapolated to thicker cells. Fig. 22 shows throughput in g/h *versus* cell thickness for two kinds of sample streams. The first kind of stream is very thin in width, less than the inside diameter of a collection tube, and this width is kept constant. The height of the stream varies with the cell thickness. This kind of stream would be used when resolution of components is the main concern, recalling the criterion for separation resolution. The second kind of sample stream is round in cross section and its diameter is *ca.* 80% of the cell thickness. This kind of stream would be used when high throughput of sample is the objective. Comparing the two kinds of streams, at 10% sample concentration in a 10-mm thick hypothetical cell, the increase in throughput from the rectangular cross section to the round cross section would be greater than a factor of 20.
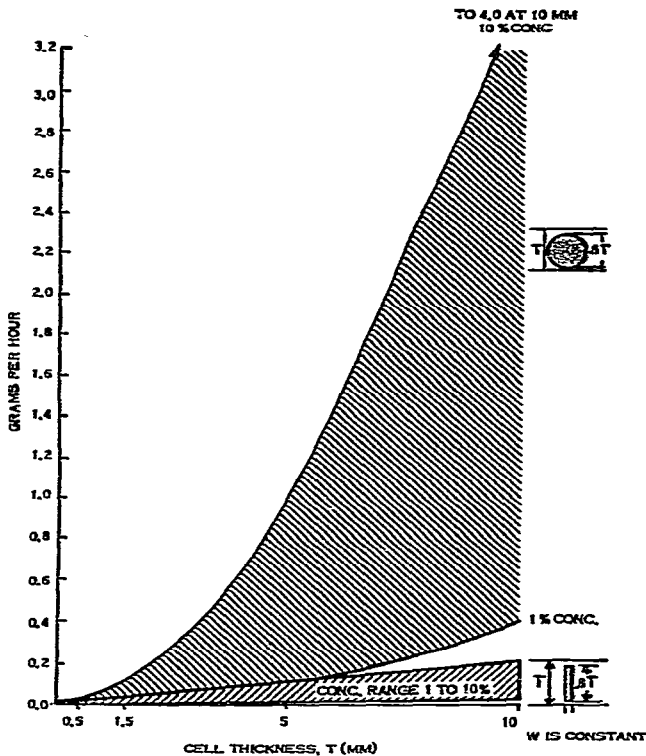
Fig. 22. Throughput *vs.* cell thickness. Lower curves represent sample concentrations for high resolution. Upper curves represent sample concentrations for maximum throughput.

CONCLUSIONS

A mathematical model of an electrophoresis cell operating under conditions of no convection and no sedimentation has been assembled. Through the use of computers, the complex interactions of the various parameters are able to be modeled realistically. The temperature gradient is probably the most important factor affecting a given separation, since this directly affects the buffer curtain profile and the electro-osmotic profile through the temperature dependence of the fluid viscosity. For a cell of given length and width, the thickness has the most profound effect on the temperature gradient since the heat transfer occurs through this dimension. For temperature stability a thinner cell is advisable. However, the buffer profile and electro-osmotic profiles are adversely affected in thinner cells except under special circumstances[7,8]. Therefore, a trade-off must be made between temperature and the two flows for systems operating in 1g environments. If the problem of convection in thick cell systems is eliminated by operation in a zero g environment the upper limit for cell thickness is governed by the maximum temperature the sample can withstand. In this way, the buffer curtain profile and electro-osmotic profile are kept as flat as possible.

Sedimentation of sample at high concentrations is another problem which plagues terrestrial free flow electrophoresis systems. By operating the system in zero g, the sedimentation of sample is negligible, allowing higher throughput.

When the inputs to the model correspond to existing equipment, the theoretical results of the model compare favorably with actual data. These results provide the basis for predicting the separation, separation resolution and throughput for thick cell systems to be operated in a zero g environment.

ACKNOWLEDGEMENT

REFERENCES

1 O. Lodge, *Brit. Ass. Adv. Sci. Rep., 56th Meeting*, London, p. 389 (1886).
2 H. Picton and S. E. Linder, *J. Chem. Soc.*, 61 (1892) 48.
3 A. Tiselius, *Trans. Farad. Soc.*, 33 (1937) 524.
4 J. Barrollier, E. Watzke and H. Gibian, *Z. Naturforsch.*, 13 (1958) 754.
5 K. Hannig, *Z. Anal. Chem.*, 181 (1961) 244.
6 A. Kolin, *Proc. Nat. Acad. Sci. U.S.*, 46 (1960) 509.
7 A. Strickler and T. Sacks, *Ann. N.Y. Acad. Sci.*, 209 (1973) 497.
8 K. Hannig, H. Wirth, B. H. Meyer and K. Zeiller, *Hoppe-Seyler's Z. Physiol. Chem.*, 356 (1975) 1209.
9 P. Debye and E. Hückel, *Phys. Z.*, 24 (1923) 305.
10 R. Audubert, *Compt. Rend. Acad. Sci. (Paris)*, 195 (1932) 316.
11 G. Gouy, *Ann. Phys.*, 7 (1917) 129.
12 D. L. Chapman, *Phil. Mag.*, 25 (1913) 475.
13 O. Stern, *Z. Elektrochem.*, 30 (1924) 508.
14 A. L. Loeb, J. Th. G. Overbeek and P. H. Wiersema, *The Electrical Double Layer Around A, Spherical Colloid Particle*, MIT Press, Cambridge, Mass., 1961.
15 P. H. Wiersema, A. L. Loeb and J. Th. G. Overbeek, *J. Colloid Interface Sci.*, 22 (1976) 78.
16 J. Th. G. Overbeek and J. Lijklema, in M. Bier (Editor), *Electrophoresis*, Vol. I, Academic Press, New York, 1959, p. 1.
17 J. Th. G. Overbeek and P. H. Wiersema, in M. Bier (Editor), *Electrophoresis*, Vol. II, Academic Press, New York, 1961, p. 1.
18 J. Th. G. Overbeek, *Advan. Colloid Sci.*, 3 (1950) 97.
19 C. C. Brinton, Jr. and M. A. Lauffer, in M. Bier (Editor), *Electrophoresis*, Vol. I, Academic Press, New York, 1959, p. 427.
20 T. W. Nee, *J. Chromatogr.*, 105 (1975) 231.
21 J. F. Brown and J. O. N. Hinckley, *J. Chromatogr.*, 109 (1975) 218.
22 Rohsenow and Hartnett, *Handbook of Heat Transfer*, McGraw-Hill, New York, 1973, pp. 7–114.
23 W. Jost, *Diffusion*, Academic Press, New York, 1952.